ARTICLES

Solvent Induced Symmetry Breaking and Relaxation Following Charge Transfer to Solvent Excitation of Na^- in Tetrahydrofuran

Zhaohui Wang, Ofir Shoshana, Bixue Hou, and Sanford Ruhman*

Department of Physical Chemistry, and the Farkas Center for Light Induced Processes, the Hebrew University, Jerusalem 91904, Israel

Received: November 27, 2001; In Final Form: January 9, 2003

Pulses of 30 fs are used to follow the dynamics of charge-transfer to solvent (CTTS) in Na^- dissolved in tetrahydrofuran (THF). The photobleach of this transition is demonstrated to be orientationally anisotropic, indicating that the CTTS band consists of a number of orthogonally oriented transitions. The pronounced anisotropy of the bleach demonstrates that interaction with the solvent orients the transition dipoles, presumably by breaking the spherical symmetry which characterizes the isotropically absorbing $Na^-_{(g)}$. The duration of solvent induced symmetry breaking was measured, and it was shown to persist for more than a picosecond. Rapid changes both in absorption and its anisotropy, which were not reported earlier, are apparent throughout the visible and near-IR. These are interpreted to reflect the presence of a primary photoproduct—tentatively assigned as the CTTS excited state, which decays completely within 200 fs. Assignment of later intermediates, analyzing the source of absorption anisotropies, and understanding the role played by the solvent in molding the photoinduced dynamics of sodide in THF are discussed.

Introduction

In the gas phase, the threshold for photoejection of an electron from $Na^-_{(g)}$ is ∼0.5 eV.[1] The spectrum for this process is nearly featureless, with residual fine structure due to autoionizing resonances related with higher ionization continua.[2,3] Solvation of the sodium anion in polar organic solvents such as ethers and amines gives rise to an intense absorption band which extends from the near-IR (NIR),[4,5] and throughout the visible, peaking at 730 nm in THF at 300 K (see Figure 1). Characterized as a charge transfer to solvent (CTTS) band, its peak wavelength depends sensitively on the nature of the solvent and its thermodynamic state, and it is deemed to reflect a transition to metastable excited states supported by the solvent.[6]

Nanosecond flash photolysis experiments show that CTTS photoexcitation of Na^- induces electron ejection into the solvent, producing a solvated electron (λ_{max}(THF) = 2 μm) and a 900 nm absorbing neutral sodium species, previously identified as a $Na^+ - e^-_{solv}$ contact pair.[7,8] Furthermore, the yield of photoelectrons following excitation of Rb^- in its analogous CTTS band was found to depend significantly upon the photon energy.[9] The dynamical processes leading from the initial excited state to photoproducts were however too rapid to be observed using nanosecond time resolution.

The intimate participation of the solvent in defining the energetics, the structure, and presumably also the ensuing dynamics suggests that CTTS photoejection constitutes an instructive example of solvent controlled nonadiabatic processes.

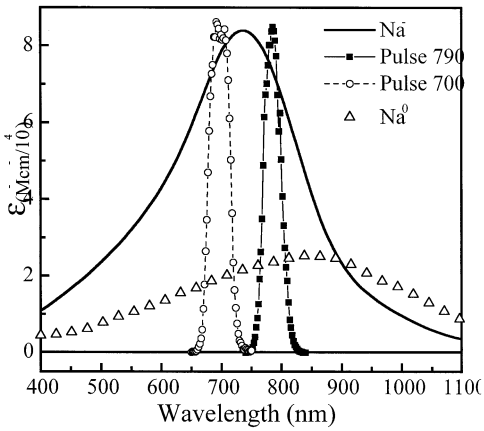

Figure 1. Absorption spectrum of sodide in THF which was used in our experiments along with spectra of the excitation pulses at 790 and 700 nm used in our experiments.

For this reason, elucidating the precise chronology of events leading to the actual transfer of charge has been the subject of recent investigation. Much of this work has concentrated on related transitions in aqueous halide solutions.[10,11] Quantum simulations of CTTS dynamics in ($I^-_{(aq)}$) portray a complex scenario which includes multiple ionization channels and relaxation pathways.[12,13] Common to all theoretical descriptions is a significant lifetime of the CTTS excited state, leading to delayed formation of electrons which are ejected in close proximity to the anion core. Bradforth and co-workers have attacked this problem experimentally by following the process

* To whom correspondence should be addressed.

10.1021/jp014331p CCC: $25.00 © 2003 American Chemical Society
Published on Web 04/05/2003

of electron ejection following CTTS excitation of aqueous iodide.[14] Their interpretation supports the predictions of relatively long-lived excited states and electron ejection in close proximity to the ion.

Schwartz and co-workers have recently addressed these same issues by investigating a related system—CTTS dynamics of Na^- in THF.[15] Using tunable pump−probe spectroscopy with an ~200 fs time resolution, transient transmission changes were probed in the visible and NIR after exciting the sample at various wavelengths. The concentration of solvated electrons was probed following excitation of Na^- in THF at 500 nm, and it was reported to rise gradually within a picosecond. Following excitation, a transient species absorbing strongly at ~600 nm was observed, disappearing within ~1 ps, leading to the products identified in nanosecond experiments. Recombination kinetics were strongly dependent upon the photodetachment wavelength and could not be rationalized with an Onsager geminate recombination model.[16] In particular, one photon excitation at 790 nm led to nearly complete geminate recombination on picosecond time scales.

The transient transmission following 500 nm excitation was interpreted with a four-state kinetic model summarized in Scheme 1, whereby excitation generates a CTTS excited state [Na^-*] absorbing strongly in the visible ($\lambda_{max} \sim 600$ nm):

SCHEME 1

$Na^- + h\nu \rightarrow (Na^-)^*$

$(Na^-)^* \rightarrow (Na^0 \cdot e^-)$ CTTS, producing a contacted pair, probability $P < 1$

$(Na^-)^* \rightarrow Na^0 + e^-$ CTTS, producing a separated pair, probability $1 - P$

$(Na^0 \cdot e^-) \rightarrow Na^-$ Recombination of contact pairs, $\tau \sim 1.0$ ps

$Na^0 + e^- \rightarrow Na^-$ Geminate recombination of separated pairs, $\tau \sim 300$ ps

The excited state then decays with a 0.7 ps time constant to produce the neutral intermediate absorbing in the NIR,[17] itself either as a contact pair with the ejected electron or in isolation. The relative abundance of contacted and separated pairs was shown to be dependent upon the excitation photons energy. Higher frequency photons produced more of the separated pairs, which were much slower to recombine.[16] Schwartz and co-workers suggest that the associations of the cations and electrons in the 900 nm absorbing neutral species are much stronger than the above definition would imply. Later three pulse experiments from their lab were interpreted as upholding the general conceptual picture embodied in Scheme 1.[18] Two rate constants were found to provide a satisfactory fit to 500 nm excitation data and lead to the spectrum of the metastable intermediate Na^-*. While some deviations of the data from the kinetic scheme were observed, no obvious experimental evidence for involvement of solvent relaxation, or continuous spectral shifts due to inherently "dynamic" evolution, was uncovered in those experiments.

Despite its success in fitting the data, as pointed out by the authors, this model is oversimplistic. The solvent is known to be strongly involved in defining the absorption spectra of Na^- and of the solvated electron. The redistribution of charge both in the CTTS excited state and even more so in the separated solvated electron cation pair must induce reorganizations of the surrounding solvent, leading to continuous changes in the absorption of the nascent products. As in most polar molecular liquids, dielectric relaxation of pure THF consists of a subpicosecond inertial component and a diffusive tail decaying within ~1.5 ps of similar amplitude.[19] Accordingly, both components should contribute to accommodation of changes in the charge distribution by the solvent and be observable in the transient spectroscopy. Furthermore, all of the simulations of CTTS dynamics, albeit for the related case of halides,[12,13] exhibit continuous shifts in energy of the newly formed products which are directly attributable to the solvent response.

A problematic aspect of the interpretation embodied in Scheme 1 concerns the relaxation time of the CTTS excited state, in view of the strong dependence of the fragment escape probability on excitation wavelength. In order for the initial photon energy to have an impact on the dynamics of the electron ejection and on fragment escape, it must not be dissipated into the solvent before the stage of ionization. This requires the solvent not to dissipate excess photon energy for nearly 1 ps. The valence electrons of alkali metals, and even more so of alkali anions, are very loosely bound. Accordingly, further electronic excitation should render the valence electrons exceedingly vulnerable to rapid solvent relaxation, making the above assertion unrealistic. The 700 fs time scale proposed for the CTTS seems excessive for conservation of the photon energy, which in turn is attested to by the continuous wavelength dependence of the ionization probability and recombination dynamics.[9,15,16]

In an independently initiated investigation[20,21] we have sought to follow the photochemical dynamics of sodide in THF. Our objectives were very similar to those of the UCLA group, that is, to deepen the insight into the nature of the CTTS excited state and to follow the solvent controlled charge-transfer dynamics using ultrafast spectroscopy. Photoselective[22] transient transmission scans following $Na^-_{(THF)}$ CTTS excitation were conducted with a laser system of superior time resolution, capable of following the solvent response on all its time scales. The data collected showed a pronounced anisotropy in the transient spectra, which decays on at least two time scales.[20,23] Here those results are fully analyzed, showing that the CTTS absorption band is inhomogeneously broadened and preferentially oriented in the solution. Furthermore, a rapidly decaying intermediate, not previously reported, is suggested to be the CTTS excited state. Revisions to the CTTS schemes portrayed by Schwartz and co-workers which are necessary to accommodate our observations are discussed and summarized in an alternative scheme.

Experimental Section

Na^- in THF was prepared by vacuum distillation of the solvent and of an amalgam consisting of ~50% potassium and 50% sodium into a glass vessel already containing a small amount of dry 15-crown-5 ether.[24] Even with small amounts of crown, an inklike and opaque solution was obtained. Part of the resulting solution was transferred to a 1 mm quartz cell attached to a side arm. The final concentration was adjusted by solvent distillation between the cell and the main reservoir of the vessel. Most data were obtained with OD = 2 solutions (@ 730 nm), except that at 500 nm obtained with $OD_{(730\ nm)} = 3$. When exciting near the absorption peak at 730 nm, these high values help in reducing the effects of group velocity mismatch when pump and probe pulses differ in color, since most of the pump energy is absorbed in a thin initial portion of the 1 mm thick solution.

Excitation pulses at 790 nm were derived directly from a 30 fs multipass amplified Ti/sapphire laser system working at 1 kHz (pulse spectrum in Figure 1). A detailed description of an amplified laser system built earlier in our lab has been published elsewhere.[25] The system used for the experiments here was constructed along similar lines. The main differences were in the pumping laser of the oscillator (Millenia S) and in the stretcher and compressor design, which was based upon 1200 lines per mm gratings, with improved diffraction efficiency (~92%/Richardson Lab). The ultimate output of the laser system when pumping the amplifier with 10 mJ of 527 nm radiation was 31 fs pulses centered at 790 nm. Their bandwidth was 38 nm, and each pulse contained 0.7 mJ of energy, with a stability of ~1% peak to peak in the compressed output.

For 700 nm excitation a supercontinuum was generated by focusing 790 nm light on a 3 mm sapphire flat with a 30 cm focal length lens. The pulses were then passed through a 40 nm fwhm interference filter centered at 700 nm, producing about 40 nJ of energy. Excitation pulses of 20 fs at 600 nm were generated in a two-stage NOPA (Clark), which was pumped by 200 μJ of the amplified output at 790 nm, and produced ~15 μJ of tunable output. Probe pulses at frequencies other than 790 nm were interference filtered from a white-light continuum generated in sapphire with a 10 cm focal length lens. Dispersion in both arms was controlled using prism pairs before impinging on the sample. Time zero was precisely determined by conducting OKE scans in thin quartz flats. The NIR probe light was generated by focusing fundamental amplifier pulses through a sapphire flat, at intensities very near the damage threshold. The probe light was selected by a slit between two prisms, with blocking on the "blue" side until practically no intensity was observed through a 50 nm fwhm interference filter centered at 1000 nm. The radiation is estimated to be in the range from 1.1 to 1.3 μm, but we were unable to determine this precisely.

Results were tested for nonlinear pump power and solution concentration dependencies, with negative results. Concentrations tested ranged from 4×10^{-4} to 6×10^{-5} M ($OD_{730\ nm} = 0.5-3$). The results were also tested for dependence upon the specific sample used or upon aging of the sample. None of the signals collected was found to change observably from one sample to another or upon aging of a single sample up to an age of over 1 month. The pump spot size was determined by transmission through a pinhole to have a diameter of ~100 μm. Pulse energies were tested from 10 to 0.2 nJ per pulse, with linear changes in the total signal intensity. No change in the temporal form of the signals was observed at all the tested fluences. These also lay much below those which were shown to produce nonlinear effects in the recent study by Martini et al.[16] Only in the case of 500 nm probing was a higher fluence used. Visible pulses were measured on amplified silicon photodiodes (EG&G), and those at wavelengths above 1 μm with large area amplified InGaAs diodes (ν-focus). The pump (chopped at 500 Hz), probe, and probe reference were digitized pulse by pulse. The differential transient transmission signal was obtained by lock-in amplification of the probe minus reference, and normalized to changes in the pump and probe energies.

Results

Due to the inevitable sample depth, only a degenerate pump−probe wavelength combination can utilize the full time resolution of our laser source. Figure 2 presents transient transmission data

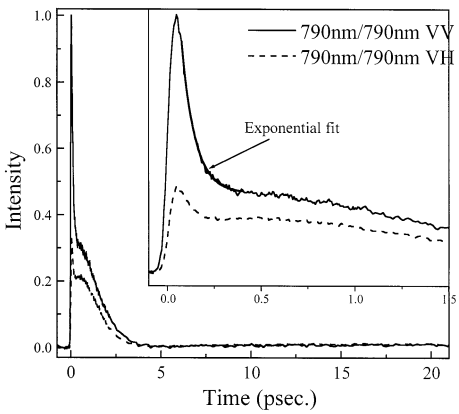

Figure 2. Transient transmission data obtained for Na^- in THF, with excitation and probing pulses at 790 nm, for the VV and VH relative polarization geometries. The inset depicts the initial 1.4 ps of probe delay.

at 790, for both VV and VH relative pulse polarizations. An instantaneous increase of transmission is observed, which is nearly 3 times more intense in the VV than in the VH. The rise is symmetrically situated with respect to the zero of delay, suggesting that it is not primarily due to a coherence spike resulting from the degeneracy of pump and probe frequencies.[26] A very rapid decay of the bleach follows, which is complete within 200 fs, and is accompanied with a reduction of the VV/VH signal ratio from 3 to ~1.25. An exponential fit to the decay of this feature results in a 1/e time of ~80 fs. No convolution with a machine response has been used here. Using a differential of the signal rise as an estimate of the cross-correlation, it became clear that it is so fast as to have negligible effect on the decay of the signal—even with $\tau \sim 80$ fs. Following this, the evolution of absorption almost levels off for about 0.5 ps. Later a slower and nearly complete regeneration of the OD commences. It is accompanied by a coalescence of the VV and VH data at ~2.5 ps. Following the transmission dip almost to its initial value at ~3 ps, it later rises gradually with a 2 ps relaxation time to an asymptotic level which reflects a ~7% long-term bleach.

To get a complete picture of the transient spectral changes following 790 nm excitation, data were collected at a series of other probe frequencies. Six of these are presented in Figures 3 and 4, covering the first 2 and 20 ps of transmission changes in both VV and VH polarization geometries, respectively. Starting with results of probing at 850 nm, to the "red" of the excitation pulse at 790 nm, the data look very similar to the 790 nm data. Some differences can be assigned to the lesser time resolution of this experiment due to the pump and probe group velocity mismatch. Again the bleach is more intense in VV probing polarization throughout the initial period of anisotropy. The rapidly decaying excess bleach which was observed at 790 nm is also observable here, albeit with lesser intensity. This must partly be due to the reduced time resolution due to the different central frequencies of the pump and probe, but it may also reflect the presence of a signal component specific to degenerate pump−probe conditions. Another difference is the deepness of the transmission dip at 3.5 ps, which actually renders the overall differential transmission signal to be negative for delays from 2 to 9 ps. Finally the delayed recovery of the bleach at later times is more pronounced here than at 790 nm.

At the other extreme of the probed range, parts of the transmission trends are similar to the NIR data. Instead of the rapid rise and fall of the bleach, at 500 nm the bleach rises more slowly, attaining its peak intensity only near a delay of

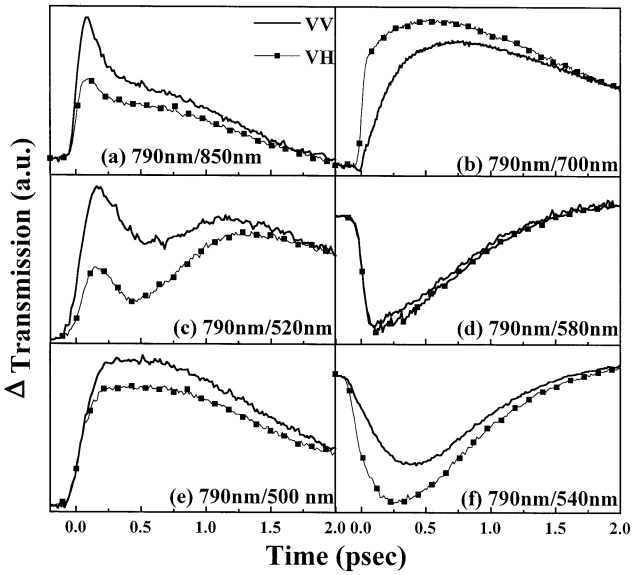

Figure 3. Transient transmission scans obtained at a variety of probing wavelengths following excitation at $t = 0$ with 790 nm pulses.

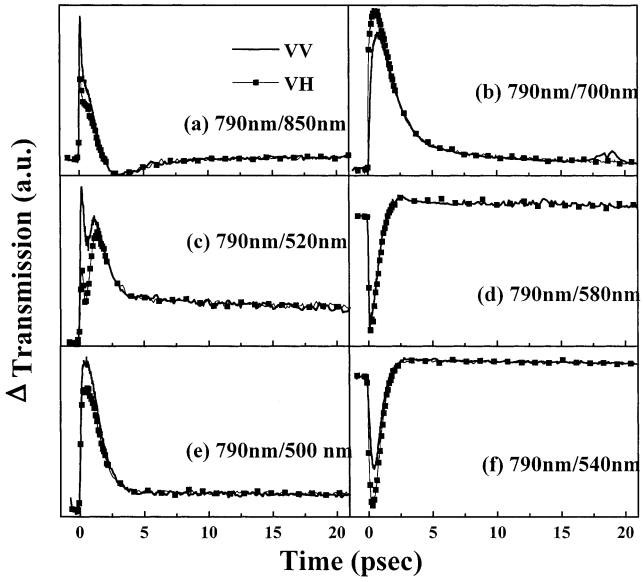

Figure 4. As in Figure 3, but data extending to delay times of 20 ps.

200 fs. From this point onward, the decay kinetics of the bleach itself and that of its anisotropy are similar at the two wavelengths. At later times the slower relaxation processes described previously at delays beyond 4 ps are not detected in the 500 nm data.

At all wavelengths in between, evidence exists for the formation of a short-lived absorbing species. This is most clearly observed near 590 nm, which is the peak wavelength associated by Barthel et al. with the CTTS excited state.[15] The initial increase in OD later gives way to a net bleach and finally exhibits a gradual asymptotic restoration of absorption at delays > 3 ps.

Striking shifts in the absorption anisotropies as the probe wavelength is tuned are revealed from the multiple wavelength data. From 780 and to the red as stated, the VV induced bleach overshadows that measured with VH relative polarizations at all delays. With 700 nm probe pulses, this ordering is reversed, and the VH transient OD is at all delays smaller than that for parallel probing. This switched ordering of OD's for VV and VH probing holds true for wavelengths from 700 nm and to

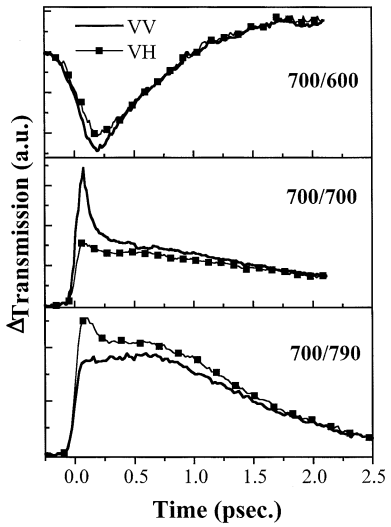

Figure 5. Transmission data at 850, 790, and 700 nm following photolysis at $t = 0$ with excitation pulses centered at 700 nm.

the blue, but the bleach anisotropy gradually diminishes so that at 580 nm the transient absorption is essentially isotropic at all delays. Further to the "blue" the ΔOD_{VV} is again smaller than ΔOD_{VH}, as observed in the data presented for probing at 500−540 nm. The relaxation of the anisotropy leads to coalescence of the VV and VH data to within the noise level at delays of ~2.5 ps for all the probed wavelengths. This issue will be dealt with quantitatively in the Discussion.

Data obtained by probing 520−540 nm data at 700 nm are particularly revealing. Aside from the unusual reversals in the sign of anisotropy between the former and the later two, they exhibit nonmonotonic transmission changes in the course of relaxation even beyond 200 fs. Considering the changes in transmission after the effects of the anisotropy are eliminated by calculating magic angle transmission changes

$$\Delta I_{MA} = \Delta I_{VV} + 2\Delta I_{VH} \quad (1)$$

the 700 nm is a bleach throughout, which increases for the first 0.5 ps of delay. At 540 as well as 520 nm, a matching rise in *absorption* over the initial 500 fs is apparent. After this delay time both trends turn around. As these wavelengths bracket the transient 600 nm transition, the shifts described above amount to a gradual and continuous 0.5 ps blue shifting of the transient absorption.

To unravel the mechanism underlying the anisotropy in transmission and its dependence upon probing wavelength, experiments were conducted with excitation pulses centered at 700 nm as well (see Figure 1 for excitation pulse spectra). VV and VH transient transmission scans at 790, 700, and 600 nm, after excitation at 700 nm, are depicted in Figure 5. The anisotropy trends are precisely reversed with respect to those of the 790 nm excitation. As before, the instantaneous bleach and its anisotropy are highest when pump and probe are degenerate, and the rapid relaxation strongly diminishes the latter. Unlike the case of 790 nm pumping, there is no direct evidence for a transient absorption component when probing at 700 nm. At 600 nm, VV and VH scans are nearly identical.

Comparing results with 790 and 700 nm pump pulses, we observe that an initial rapidly relaxing excess bleach is observed at all probing wavelengths which lie to the "red" with respect to the pumping frequency. To further investigate this point, data were collected with $\lambda_{pump} = 600$ nm as well. The above

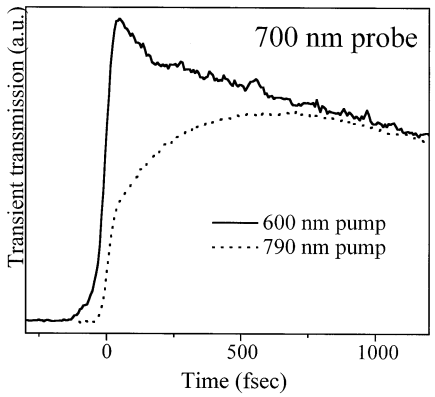

Figure 6. Transient transmission scans with delays from 0 to 2 ps, probing at 700 nm, the former with 790 nm and the latter with 600 nm pump pulses, respectively.

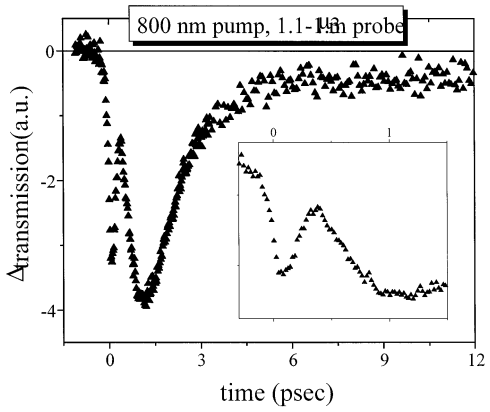

Figure 7. VV transmission scan of a sodide solution, pumping with 790 nm pulses, and probing with NIR probe radiation generated as discussed in the Experimental Section.

statement held true for this excitation wavelength as well. To demonstrate this, we present in Figure 6 two scans from 0 to 2 ps, both probing at 700 nm, the former with 790 nm and the later with 600 nm pump pulses, respectively. This is the only probing wavelength for which we have data for pump frequencies lying both to the "blue" and to the "red".

Finally, in a first effort at probing transmission changes in the NIR, data were collected for 790 nm pump pulses and probe radiation generated as described in the Experimental Section. Results are shown only for the VV geometry in Figure 7. In the NIR a very fast initial feature is also observed, but it appears as an absorption, not a bleach or emission. Later a slower rise and subsequent decay are evident, peaking at about 1 ps. Very slight anisotropies were observed here also at early times, but they are complicated by involvement of numerous contributing intermediates and will not be presented here.

Discussion

Rationalizing of the data is initiated in terms of Scheme 1. As described in the previous section, signals detected well above or below 600 nm, where the CTTS excited state is purported to absorb, exhibit common trends in transient transmission. The reduction of OD agrees with the disappearance of the sodide reactant and generation of intermediates of lesser absorbance (Na^0, e^-_{solv}). As probing approaches 600 nm, absorption of the intermediate previously identified as the CTTS excited state overwhelms the parent bleach and leads to net absorptions immediately following irradiation, all the way from 540 to 640 nm. Invariantly, this trend is later reversed to a net bleach which itself reduces with time together with that outside the absorption range, due mainly to recombination and reformation of the highly absorbing initial reactant.

Along with these trends, a number of significant new observations are reported above which need to be discussed and ultimately incorporated into a reactive scheme describing Na^- photochemistry. The most unusual of these observations is the substantial anisotropy in the transient spectra, with its intricate reversal of sign as the probing wavelength is tuned. Another is the ultrafast initial relaxation process, which reveals itself in rapid shifts of absorption and absorption anisotropy during the first ~200 fs after photoexcitation. Discussion will begin by scrutinizing the newly revealed absorption anisotropy. Conclusive arguments will be provided to show not only that the prolonged anisotropy stems from a single species but also that it can be assigned solely to anisotropy in the bleach of the reactant ions absorption. Later, the initial rapid relaxation processes will be examined, and finally, continuous solvent induced relaxation processes for which we find evidence in the transient spectroscopy will briefly be discussed.

(a) Assignment of the Observed Transmission Anisotropy. Given the overlapping of the reactant absorption spectra with those of various reactive intermediates, interpretation of the observed anisotropy must begin by identifying its source. The magnitude of this anisotropy reduces markedly with the initial relaxation process but does persist quite a bit beyond that point. We start by assigning the anisotropy which survives for $t \geq 200$ fs, and we leave for later the earlier features. The two valence electrons in sodide lead to a strongly dipole allowed s−p transition as the lowest electronic excitation. In isolation, due to its spherical symmetry, absorption from the s state should be equally probable for light polarized in any direction. Accordingly, the bleach of such a transition, even when induced by linearly polarized light, will also be isotropic and retain no record of the orientation in space of the field vector which induced the transition, after the electronic coherence is dephased. This will not be true of transient absorption or emission from an isolated excited p state, which may retain the polarization of the exciting light much beyond that point.

When dealing with spectroscopic anisotropy due to a single transition, one can calculate the degree of alignment of the relevant transition moment using eq 2:

$$r(t) = (\Delta I_{VV} - \Delta I_{VH})/(\Delta I_{VV} + 2\Delta I_{VH}) = C\langle P_2(\cos(\theta))\rangle \quad (2)$$

ΔI represents the differential amplitude of absorption or emission related with the transition. P_2 is the second Legendre polynomial of the angle between the orienting dipole at time zero and at time t, and C is a constant depending on the relative directions of the orienting dipole and the probing one.[22] $(\Delta I_{VV} + 2\Delta I_{VH})$ represents an orientationally averaged change in OD such that $(\Delta I_{VV} + 2\Delta I_{VH}) \propto \Delta_C \epsilon_\lambda l$, where Δ_C is the change in concentration of the optically active species and ϵ_λ is its extinction coefficient at the probing wavelength. Clearly, with overlapping polarized transitions, such a calculation loses all physical significance. There is, however, one quantitative measure which can help in identifying the species giving rise to the absorption anisotropy, or at least in indicating if the anisotropy is due to a single species (i.e., that for all other bands $\Delta I_{VV} = \Delta I_{VH}$). When that is the case, the normalized time dependence of $(\Delta I_{VV} - \Delta I_{VH})_\lambda$ will be independent of λ. This stems directly from an evaluation of the subtraction in eq 3:

$$(\Delta I_{VV} - \Delta I_{VH})_\lambda = \sum_i C_i \langle P_2(\cos(\theta))\rangle \Delta_C (\epsilon_\lambda)_i l \quad (3)$$

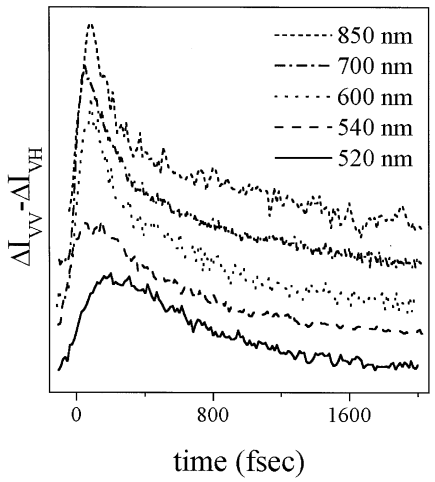

Figure 8. Plot of $(\Delta I_{VV} - \Delta I_{VH})$ for a number of probing wavelengths, normalized to its intensity at a delay of 200 fs. The various wavelengths have been offset vertically to facilitate viewing.

where the summation is over all transitions taking place from the single species. Thus, assuming the degree of alignment of the ensemble to be the same for all transitions and the extinction coefficients (negative for emission) at λ to be constant, all will be proportional to $P_2\Delta_C$, a time varying measure sensitive both to the alignment and the change in concentration of the probed species.

Results of such an analysis are presented graphically in Figure 8. Remarkably, despite the very different appearances of the transient transmission, the subtraction scans, normalized to the amplitude at ~200 fs, line up very well for *all the wavelengths probed in our experiments*! This indicates that, from 200 fs and onward, the anisotropy detected at all probed wavelengths is due to a single species. Since it must have an absorption which is very broad, and it must be formed promptly, the anisotropy in absorption must be assigned to the pump induced bleach of the reactant Na^- alone! This leads to two most important conclusions: first, that solvation of sodide in THF breaks its spherical symmetry, leading to orientation of the transition dipoles involved in the s → p absorption; and, second, that all other species absorbing and emitting at $t > 200$ fs do so *isotropically*—and retain no preferred orientation from the initial pump radiation.

Having identified the sodide bleach as the sole anisotropic absorber, the changes in sign of $(\Delta I_{VV} - \Delta I_{VH})$ as λ_{probe} is varied indicate that the CTTS absorption band consists of a number of overlapping transitions which have dipoles which are orthogonally oriented. This is often the case for s → p excitation centers in condensed media which have been distorted from perfect spherical symmetry, such as Jahn−Teller vibronic distortions in crystals.[27] In this scenario, an elongation in the solvent cage reduces the electronic energy of a p orbital directed along the distortion axis with respect to that of another orbital polarized at right angles to it. This removes the degeneracy of the s → p manifold and produces at least two orthogonally polarized bands. Just such a scenario was predicted theoretically by Rossky and co-workers for the photophysics of hydrated electrons[28]and later, inspired in part by our results, by Jungwirth and Bradforth[29] for CTTS spectra of iodide in water. Despite early reports that experiments upheld the theoretical predictions for the electron,[30] the results later came under question, and the issue has yet to be resolved.[31] In view of the ongoing controversy, it is most significant that such a clear case of solvent induced symmetry breaking *is* observed in this closely related system.

(b) Asignment of the $t < 200$ fs Relaxation. A glance at Figure 8 shows that even before $t = 200$ fs the normalized anisotropy is identical for all delay times in nondegenerate pump−probe data from 600 nm to the NIR. The subtraction signal decays biexponentially, with the first phase characterized by $\tau \sim 100$ fs and the slower phase having $\tau \sim 700$ fs. In the degenerate case, the two phases of decay are conserved with the fast component much larger in amplitude. When probing further to the blue, $(\Delta I_{VV} - \Delta I_{VH})$ differs in appearance, with the initial decay showing up as a rise. The biphasic decay is just one of numerous manifestations of a substantial dynamic process taking place within the first 200 fs in this system, including the reported excess bleach at the pumping frequency, also observed with lesser amplitude when probing to the red of the pump, and another being the equally short-lived absorption feature in the NIR.

One might interpret Figure 8 as indicating that the two lowest energy bands in the CTTS manifold (NIR-730 nm, 730−600 nm) are due to a single species at all times, whereas the absorption to the blue arises from a closely related species, connected by an extremely rapid dynamic process to the former, which acts to redistribute the impulsive bleach throughout the full CTTS manifold. Also, it seems clear that at least some of the initial bleach intensity must be specific to spectrally degenerate conditions. However, in view of the wavelength dependent time resolution obtained in the thick sample, due to group velocity mismatch of pump and probe, such a conclusion is premature. Less specifically, the early pump−probe data, especially the rapid reduction of anisotropy, could equally be due to dephasing of the impulsively excited transition dipole[32] or to the photodetachment of the ions excess electron.

At this stage we choose to promote the later of these assignments, that is, that the rapid relaxation reflects the stage of photoionization, due to its consistency with all the experimental observations, including those of a three-pulse experiment recently disclosed, preliminarily:[21]

(1) A very brief ionization is compatible with the strong wavelength effect on the probability for generating separated electron−atom pairs. If the ejection is prompt enough, the solvent will not have time to take up the excess photon energy, which will in turn be effective in energizing the leaving electron.

(2) The rapid relaxation stage gives rise to an intermediate which absorbs *isotropically* in the visible, that is, has lost memory of the pump polarization—*just as would be expected following a reactive stage such as photodetachment*!

(3) Within this framework, the 600 nm absorbing intermediate supersedes ionization and is accordingly a neutral sodium species. Its narrow absorption in the midvisible—just where isolated sodium atoms absorb—matches this interpretation naturally.

(4) The NIR absorption in Figure 7 arises from only two species—the solvated electron e^- and, more pronouncedly, $(Na^0)_{solv}$ absorbing broadly at 900 nm. Since they appear as matched intermediates in Scheme 1 (i.e. are formed and consumed together, at a 1:1 ratio), their absorptions should rise and decay with identical kinetics. Comparing Figure 7 with 2 μm probing from the literature[15] shows a very different trend, where the ~1.2 μm data peak much later than the electron band—indicating that at least one kinetic stage must separate them in a correct reactive scheme.

(5) The short-lived excess bleach always observed to the "red" of the exciting pulse wavelength is compatible with a short-lived emission from a nascent excited state.

All of the above lead to the suggestion of an alternative model summarized in Scheme 2:

SCHEME 2

$Na^- + h\nu \rightarrow (Na^-)^*$

$(Na^-)^* \rightarrow [(Na^0)_{dry} \cdot e^-]$	CTTS, producing a contacted pair, probability $P < 1$ (<200 fs)
$(Na^-)^* \rightarrow (Na^0)_{dry} + e^-$	CTTS, producing a separated pair, probability $1 - P$ (<200 fs)
$(Na^0)_{dry} \rightarrow (Na^0)_{solv}$	900 nm absoring species
$[(Na^0)_{solv} \cdot e^-] \rightarrow Na^-$	Recombination of contact pairs, $\tau \sim 1.0$ ps
$(Na^0)_{solv} + e^- \rightarrow Na^-$	Geminate recombination of separated pairs, $\tau \sim 300$ ps

Identifying the stage of ionization is of central importance. Charge transfer in solution is often controlled by solvent fluctuations which bring the initial and final electronic states into transient degeneracy. While a 700 fs CTTS excited state lifetime might uphold such an interpretation, one of <200 fs certainly would not, since the solvent would not have time to influence the system in so short an interval. Thus, the shift in assignment of ionization timing radically alters our concept of the CTTS dynamics in this system. Thus, the shift in assignment of ionization timing radically alters our concept of the CTTS dynamics in this system. Shifting assignment of the CTTS excited state raises the question of the correct identity of the 600 nm absorbing intermediate[15] (as all subsequent intermediates are identified, this is the crux of the matter). A plausible assignment identifies the visible absorbing species as a "dry" or unsolvated neutral sodium atom. Contraction of the nascent sodium due to ejection of its excess electron may leave it in a large and noninteracting solvent cage, perhaps explaining why the neutral starts absorbing like an isolated atom. Within this scenario, the disappearance of the 600 nm absorbing species and buildup of the 900 nm band must reflect a solvent induced nonadiabatic change in the electronic state of the neutral brought on by solvation, the most plausible being spontaneous ejection of an additional electron to form a closely bound sodium cation−electron "ion pair". How solvent induced blue shifting of the 600 nm band can be compatible with its facilitating a nonadiabatic change in the electronic state to produce $(Na^0)_{solv}$ will be discussed presently.

(c) Possible Spectral Manifestations of Solvent Induced Relaxation. In the description of the results, indication was given to a blue shifting of the absorption we assign to a "dry" sodium atom. Absorption of a nascent photoproduct which is formed out of the solvation equilibrium is expected to exhibit anti-Stokes shifting due to solvent relaxation when probed through absorption, just as this leads to a dynamical Stokes shifting when observed by emission. This interpretation does not lead to a precise determination of solvation dynamics, since the resulting blue shifting coincides with a number of dynamical processes, such as electron ejection, product solvation, and recombination, which simultaneously influence the absorption. We note in passing that solvent induced energy relaxation and nonadiabatic curve crossings, such as those envisioned in populating $Na^0{}_{solv}$, are not mutually exclusive, since adiabatic evolution takes place before and after sudden nonadiabatic potential hops.

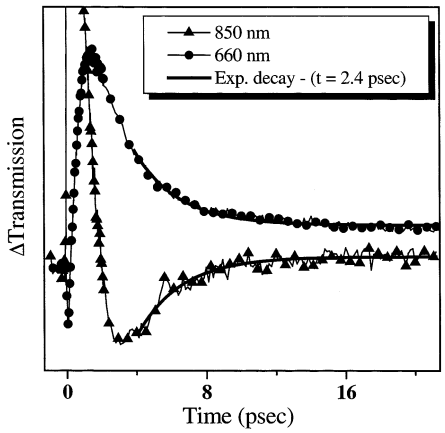

Figure 9. Exponential analysis of the long-term spectral decays at 850 and 680 nm, using the same decay time of 2.4 ps.

On the other hand, the slow final shifts in OD at $t > 4$ ps, showing up above and below the peak of Na^- absorption, may present another opportunity. To the blue of λ_{max} at 730 nm, a gradual restoration of absorption is observed, whereas to the red, on precisely the same time scale, excess absorption disappears, again constituting a blue shift of the sodide absorption band. When fitting this portion of the data to a single exponential, decay times ranging from 2 to 2.4 ps are obtained—similar to the longer dielectric relaxation time in THF (1.5 ps). This is demonstrated for two wavelengths in Figure 9. The interpretation of these spectral changes as solvation is based upon the observation that simultaneously transmission scans at 500−540 nm are perfectly flat—indicating that the rapid recombination is over and no changes in the concentrations of the various intermediates are taking place. This reasoning has to be taken with a grain of salt until the anisotropy differences observed in these two spectral ranges are fully clarified. More detailed experiments must be devised to investigate this and how the neutral sodium atom can exist in such very different states in the liquid. Experiments using a 200 μm cell are underway to clarify these points.

One would also like to gain insight into the degree of asymmetry required in the solvation shell for splitting the p bands by a few thousand inverse centimeters and to seek corroborating evidence for the assignments of the early intermediates in this reaction, particularly for the species absorbing centered at 600 and 900 nm. Regardless of discrepancies which seem at present to exist between MD simulation predictions and photoselective hole-burning experiments in the case of the hydrated electron, it seems that theory will be the most straightforward way of estimating these points. In any case, the ongoing experiments to detect the appearance of electron absorption with high time resolution should contribute to resolving these issues as well.

Conclusions

Application of high time resolution photoselective flash photolysis to sodide in THF uncovers new and unusual characteristics of this system. Na^- in isolation is an isotropically absorbing two valence electron atom. Its introduction into the solvent breaks the spherical symmetry of the ion and orients the transition dipoles, which are associated with the CTTS band. Furthermore, this broad band is made up of several underlying transitions, as attested to by the change in sign of $(\Delta I_{VV} - \Delta I_{VH})$ as the probe or pump frequencies are tuned. An ultrafast stage of spectroscopic change, both in differential transmission and

in its anisotropy, which is completed in ~200 fs, is observed here for the first time and assigned to decay of the CTTS excited state by electron ejection. We conclude that the metastable species absorbing at ~600 nm after CTTS excitation is not, as earlier thought, the CTTS excited state. It is alternatively assigned as neutral sodium which is not completely solvated. Direct demonstration of this assignment and full characterization of the CTTS dynamics await the results of ongoing experiments which directly probe the electron appearance with higher time resolution using ultrathin sample cells and theoretical simulations which include specific solvent−solute interactions.

Acknowledgment. We thank J. Dye and M. J. Wagner for helpful suggestions, and the groups of M. Rabinovitch and H. Levanon for technical assistance in preparing our samples. We thank P. Rossky and S. Bradforth for enlightening discussions, and we acknowledge receipt of manuscripts from B. Schwartz prior to publication. Help from E. Riedle and J. Piel with NOPA setup is gratefully acknowledged. This research was supported by the U.S.−Israeli binational science foundation, and the James Franck program for laser matter interactions. The Farkas center is funded by the Minerva Gesellschaft, GmbH, Munich, Germany.

References and Notes

(1) Liu, C.-N.; Strance, A. F. *Phys. Rev. A* **1999**, *59*, 3643.
(2) Haeffler, G.; Kiyan, I. Y.; Hanstorp, D.; Davies, B. J.; Pegg, D. J. *Phys. Rev. A* **1999**, *59*, 3655.
(3) Dye, J. L. *Prog. Inorg. Chem.* **1984**, *32*, 327.
(4) Dye, J. L.; Dewald, J. L. *J. Phys. Chem.* **1964**, *68*, 135.
(5) Ottolenghi, M.; Bar-eli, K.; Linschitz, H.; Tuttle, T. R., Jr. *J. Chem. Phys*. **1964**, *40*, 3729. Gaathon, A.; Ottolenghi, M. *J. Phys. Chem*. **1969**, *73*, 3039.
(6) Matalon, S.; Golden, S.; Ottolenghi, M. *J. Phys. Chem*. **1969**, *73*, 3098.
(7) Gaathon, A.; Ottolenghi, M. *Isr. J. Chem.* **1970**, *8*, 165.
(8) Huppert, D.; Bar-Eli, K. H. *J. Phys. Chem.* **1970**, *74*, 3285.
(9) Rozenshtein, V.; Heimlich, Y.; Levanon, H.; Lukin, L. *J. Phys. Chem. A* **2001**, *105*, 3701.
(10) Blandamer, M. J.; Fox, M. J. *Chem. Rev.* **1970**, *70*, 59.
(11) Jortner, J.; Ottolenghi, M.; Stein, G. *J. Phys. Chem.* **1964**, *68*, 247.
(12) Sheu, W. S.; Rossky, P. J. *J. Phys. Chem.* **1996**, *100*, 1295.
(13) Staib, A.; Borgis, D. *J. Chem. Phys.* **1996**, *104*, 9027.
(14) Kloepfer, J. A.; Vilchiz, V. H.; Lenchenkov, V. H.; Bradforth, S. E. *Chem Phys. Lett.* **1998**, *298*, 120. Kloepfer, J. A.; Vilchiz, V. H.; Lenchenkov, V. A.; Germaine, A. C.; Bradforth, S. E. *J. Chem. Phys.* **2000**, *113*, 6288.
(15) Barthel, E. R.; Martini, I. B.; Schwartz, B. J. *J. Chem. Phys.* **2000,** *112*, 9433. Barthel, E. R.; Martini, I. B.; Schwartz, B. J. *J. Phys. Chem. B* **2001**, *105*, 12230.
(16) Martini, I. B.; Barthel, E. R.; Schwartz, B. J. *J. Chem. Phys.* **2000**, *113*, 11245.
(17) Piotr, P.; Miller, J. R. *J. Am. Chem. Soc.* **1991**, *113*, 5086.
(18) Martini, I. B.; Barthel, E. R.; Schwartz, B. J. *J. Am. Chem. Soc.* **2002**, *124*, 7622. Martini, I. B.; Schwartz, B. J. *Chem. Phys. Lett.* **2002**, *360*, 22.
(19) Reynolds, L.; Gardecki, J. A.; Frankland, S. J. V.; Horng, M. L.; Maroncelli, M. *J. Phys. Chem.* **1996**, *100*, 10337.
(20) Wang, Z.; Shoshana, O.; Ruhman, S. In *Ultrafast Phenomena XII*; Elsaesser, T., Mukamel, S., Murnane, M. M., Scherer, N. F., Eds.; Springer series in chemical physics 66; Springer-Verlag: Heidelberg, 2001; pp 624−626.
(21) Sension, R.; Wang, Z.; Shoshana, O.; Hou, B.; Ruhman, S. In *Ultrafast Phenomena XIII*; Murnane, M. M., Scherer, N. F., Miller, R. J. D., Weiner, A. M., Eds.; Springer series in chemical physics; Springer-Verlag: in press.
(22) Albrecht, A. C. In *Progress in Reaction Kinetics*; Porter, G., Ed.; 1970; Vol. 5.
(23) The anisotropies reported in our work have been observed recently also by the UCLA group: Barthel, E. R.; Martini, I. B.; Keszei; Schwartz, B. J., in preparation.
(24) Dye, J. L. *J. Phys. Chem*. **1980**, *84*, 1084.
(25) Gershgoren, E.; Vala, J.; Kosloff, R.; Ruhman, S. *J. Phys. Chem. A* **2001**, *105*, 5081.
(26) Heinz, T. F.; Palfrey, S. L.; Eisenthal, K. B. *Opt. Lett.* **1984**, *9*, 359.
(27) Schwentner, N.; Koch, E. E.; Jortner, J. *Electronic excitations in condensed rare gases*; Springer Tracts, Vol. 107; Springer: Berlin, 1985. Bersuker, I. B.; Polinger, V. Z. *Vibronic interactions in Molecules and Crystals*; Springer-Verlag: 1983.
(28) Schwartz, B. J.; Rossky, P. J. *Phys. Rev. Lett.* **1994**, *72*, 3282.
(29) Bradforth, S. E.; Jungwirth, P. *J. Phys. Chem. A* **2002**, *106*, 1286.
(30) Reid, P. J.; Silva, C.; Walhout, P. K.; Barbara, P. F. *Chem. Phys. Lett.* **1994,** *228*, 658.
(31) Assel, M.; Laenen, R.; Laubereau, A. *J. Phys. Chem. A* **1998,** *102*, 2256.
(32) Wynne, K.; Hochstrasser, R. M. *J. Raman Spectrosc.* **1995**, *26*, 561.